DesignCon 2009

40/100 Gbps Transmission Over Copper, Myth and Realities

Ali Enteshari, The Pennsylvania State University
enteshari@psu.edu

Mohsen Kavehrad, The Pennsylvania State University
mkavehrad@psu.edu

Abstract

This paper focuses on assessment and design of transmission systems for distribution of digital signals over standard Category-7A copper cables at speeds beyond-10Gbps. The main contribution of this paper is on the technical feasibility and system design for data rates of 40 and 100Gbps over copper. Based on capacity analysis and rate optimization algorithms, system parameters are obtained and the design implementation trade-offs are discussed. Our simulation results confirm that with the aid of Decision-Feedback Equalizer and powerful coding techniques, e.g. TCM or LDPC code, 40Gbps transmission is feasible over 50m of CAT-7A copper cable. These results also assure that 100Gbps transmission can be achieved over 15m cables.

Authors Biography

Ali Enteshari received the B.Sc. and M.Sc. degrees in electrical engineering from Sharif University of Technology in 1999, and 2001, respectively. He is currently working toward the Ph.D. degree at the department of electrical engineering, Pennsylvania State University, University Park.

Mohsen Kavehrad received his Ph.D. degree from Polytechnic University (Brooklyn Polytechnic), November 1977, in electrical engineering. Since January 1997, he has been with the Pennsylvania State University EE Department as W.L. Weiss Chair Professor and founding Director of Center for Information and Communications Technology Research.

Introduction

In the commercial market, a new challenge is the extension of fiber into the access network in small business and dense metropolitan areas. It has long been known that a major bottleneck in delivering multimedia services to the computer users is the low-capacity of LANs. With ever-increasing demand for higher capacities, the need for broadband access is transformed from a convenience to a necessity. So far, data communication has been the main driving force behind increased traffic on the communication networks. Applications stemming from a wide range of disciplines such as high-performance computing, consumer multimedia, teleconferencing and telemedicine are just few examples that require data rates in the gigabits per second range. To keep up with this explosive growth, ultra high-capacity networks were required, and thus optical networks with terabit capacities dominated the network core. To enable the end user to take full advantage of this core, reliable high-speed LAN access is required. Providing service in a broadband access LAN, using a copper cable approach, has the advantages of network being highly-dependable and cost-effective. This will benefit the providers of service over campus settings like hospitals, industry compounds or universities with facilities spread over several buildings that a quick service upgrade could extend new service offerings. Also, within server farms and data centers, short copper connectors are preferable.

After release of the 10GBASE-T, which supports data rates of 10Gbps up to a distance of 100 meters (for connecting work areas to a telecommunications room), many IEEE members recognized the potential for higher speed and are currently thinking of ways to deliver tens of Giga bits per second over copper cables. Researchers have started to study the technical feasibility, broad market potential, and economic feasibility of speeds beyond 10Gbps over copper. In this paper, we evaluate the possibility of 40Gbps and 100Gbps data rates (40GBASE-T and 100GBASE-T) over horizontal balanced CAT-7A cables up to a distance of 50 meters. The objective of IEEE 40(100)GBASE-T is to create an application that is capable of transporting data at a rate of 40(100) Gbps over at least 10 meters of copper cable [1]. The cable industry, is promoting the use of CAT-7A cable (or better CAT-8) to support these demanding applications. It is expected that this CAT-7A cable will be characterized up to some higher frequency value determined by consensus within the IEEE 802.3 Higher speed Study Group [1]. State-of-the-art digital signal processor (DSP) will be used to cancel impairments in the twisted-pair cable and noise from the external environment to ensure adequate signal-to-noise ratio (SNR) to achieve a suggested target average bit error rate of 10^{-12} at data rates of 40Gbps and beyond [2][3].

The main contribution of this paper is in the technical feasibility assessment and system design for a data rate of 40Gbps (and 100Gbps) over copper wire. We start by multi-input multi-output (MIMO) modeling and present formulas for capacity bounds. These bounds are a good performance measure for a channel impaired by background noise and crosstalk signals. We will prove that single-input single-output (SISO) implementation will perform as good as MIMO implementation and this is due to low FEXT level in CAT-7 cables. We use the specification of CAT-7A cable, an enhanced version of CAT-7 with a better performance and engineering design, to analyze, model and finally optimize the parameters for the given system requirements.

System Model

The CAT-7A cable is made of four doubly shielded horizontal balanced twisted-pairs, labeled by Blue, Brown, Orange and Green colors, and is shown in Fig. 1. One can set up a communication system consisting of four transceivers at each end. A data stream is subsequently shaped by a pulse filter $p(t)$ and mapped onto a vector waveform $\boldsymbol{x}(t) = [x^1(t), \cdots, x^4(t)]^T$, where $x^n(t) = \sum_m x_k^n p(t - mT), n = 1, \cdots, 4$ is the input signal to the n-th channel.

Typically, signal constellations $\boldsymbol{x}_k = [x_k^1, \cdots, x_k^4]^T$ are taken from the scaled lattice $\mathbb{Z}^4$ (or D^4) [4] to maximize the minimum Euclidean distance. Category cables are designed in a way that all twisted pairs behave more or less similarly, so the total rate is divided among them equally. Therefore, x_k^n is drawn from a finite alphabet set (e.g. M-PAM signaling) that contains equidistant real symbols centered on the origin, for example,

$$\mathcal{A} = d\{\pm 1, \pm 3, \cdots, \pm (M-1)\} \tag{1}$$

where $2d$ is the minimum distance between symbols.

Assuming that the receiver synchronously samples the output of the vector channel, we can write the received sample vector at time $k\mathrm{T}$ as

$$\boldsymbol{r}_k = \mathbf{H}(t) * \boldsymbol{x}(t) + \mathbf{G}(t) * \boldsymbol{z}(t) + \boldsymbol{v}(t)\Big|_{t=k\mathrm{T}} \tag{2}$$

where $\mathbf{H}(t)$ is the matrix impulse response of the vector channel, $\boldsymbol{z}(t) = [z^1(t), \cdots, z^4(t)]^T$ is the interfering signal from the near-end transmitters, $\boldsymbol{v}(t) = [v^1(t), \cdots, v^4(t)]^T$ is the additive noise, and $*$ is the convolution operator. Generally, the near-end interferers $z^n(t) = \sum_m z_k^n p(t - mT), n = 1, \cdots, 4$ share the same statistical properties as $x^n(t)$; they are both zero-mean wide-sense stationary processes, and the 4×4 autocorrelation

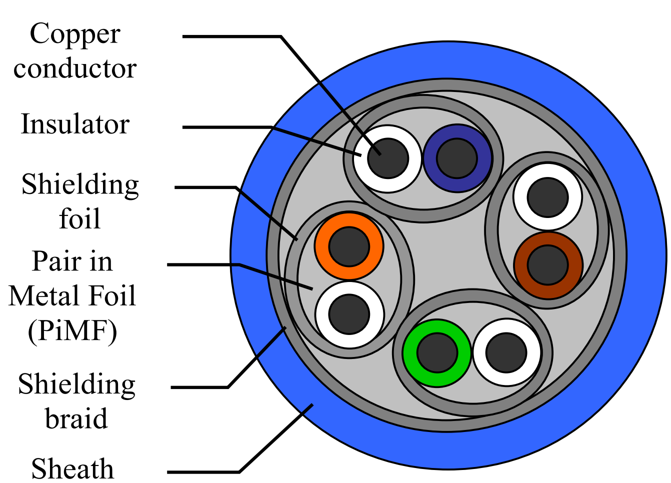

Fig. 1 Cross-section of Category 7 S/FTP cable.

matrices of x_k^n and z_k^n are given by $\mathbf{R}_{xx} = \mathbf{R}_{zz} = \overline{P}_s \mathbf{I}_4$, which means x_k^n (and z_k^n) are uncorrelated, both spatially and temporally. We also assume that the noise samples are uncorrelated, both temporally and spatially (i.e. $\mathbf{R}_v = \sigma_v^2 \mathbf{I}_4$).

The signal attenuation and electromagnetic coupling between the twisted-pairs are described by the frequency-selective multiple-channel transfer function $\mathbf{H}(t)$. The diagonal elements of $\mathbf{H}(t)$ represent insertion loss (IR), which is a measure of the decrease in signal strength along the length of a transmission line. The off-diagonal elements are pair-to-pair far-end crosstalk (FEXT) loss that quantify undesired signal coupling between adjacent pairs at the far-end of the cable. Due to proper shielding of CAT-7A cable, the alien near-end crosstalk is negligible (although, if its power is significant, it can simply be included into our model).

The near-end effect is also incorporated in this model as a frequency selective multiple channel system $\mathbf{G}(t)$, with 4 transmit and 4 receive nodes. The diagonal and off-diagonal elements of $\mathbf{G}(t)$ represent return loss (RL), and near-end crosstalk (NEXT), respectively. Pair-to-pair near-end crosstalk loss quantifies undesired signal coupling between adjacent pairs at the near-end (the same end as the transmit-end) of the cable, while return loss is a measure of the signal reflections occurring along a transmission line and related to impedance mismatch.

In vector form, eq. (2) can be written as

$$\boldsymbol{r}_k = \sum_{m=0}^{n_H} \mathrm{H}_m \boldsymbol{x}_{k-m} + \sum_{m=0}^{n_G} \mathrm{G}_m \boldsymbol{z}_{k-m} + \boldsymbol{v}_k \tag{3}$$

where it is assumed that, without loss of generality, all the elements of $\mathbf{H}$ ($\mathbf{G}$) have the same channel order n_H (n_G), and

$$\mathrm{H}_k = \begin{bmatrix} h_{1,1}[k] & \cdots & h_{1,4}(k) \\ \vdots & \ddots & \vdots \\ h_{4,1}[k] & \cdots & h_{4,4}[k] \end{bmatrix} \mathrm{G}_k = \begin{bmatrix} g_{1,1}[k] & \cdots & g_{1,4}(k) \\ \vdots & \ddots & \vdots \\ g_{4,1}[k] & \cdots & g_{4,4}[k] \end{bmatrix} \tag{4}$$

Fig. 2 depicts the insertion loss and return loss of the Blue pair ($h_{1,1}$ and $g_{1,1}$) along with the NEXT and FEXT interference signals from the Brown pair ($h_{1,2}$ and $g_{1,2}$) as functions of the frequency.

Capacity Bounds

In this section, we first review the capacity of the general Additive White Gaussian Noise (AWGN) channel, and introduce the *Single-Carrier*, *Water-filling*, SISO and MIMO capacity notations for Category cables.

As a first step toward designing any communication system, the capacity limit of the communication medium (CAT-7A) has to be determined. The channel capacity C can be calculated from the physical properties of a channel. The Shannon-Hartley theorem [5][6] states the theoretical maximum rate of *error-free* data that can be sent with a given signal

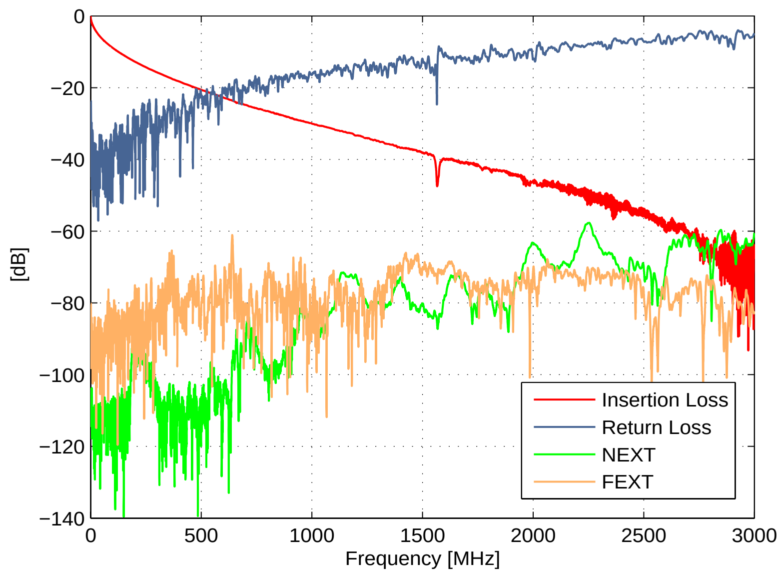

Fig. 2 Insertion Loss, Return Loss, NEXT and FEXT measurements for 50m CAT-7A.

power spectrum $S(f)$ through an analog communication channel subject to additive (possibly colored) Gaussian noise with power spectrum $V(f)$. According to this theorem, the capacity of a band-limited channel with Gaussian noise is:

$$C_{\mathrm{SH}} = \int_0^W \log_2\left(1+\frac{S(f)}{V(f)}\right)df \simeq \sum_{n=1}^{N}\frac{W}{N}\log_2\left(1+\frac{S(f_n)}{V(f_n)}\right) \tag{5}$$

where C_{SH} is the channel capacity in bits per second, W is the bandwidth of the channel in Hz, and finally f is frequency in Hz.

Over a highly dispersive channel, an efficient way to utilize the allocated bandwidth is to treat the channel through N independent sub-channels which have a nearly flat frequency response by making N large enough. It is desirable to have all sub-channels with the same probability of error, p_e. Constant p_e can take place when all sub-channels use the same class of codes with a constant SNR gap Γ. In this case, a single performance measure characterizes a multi-channel transmission system. This measure is a geometric SNR that can be compared to the detection SNR of equalized transmission systems. The asymptotic capacity of this multi-channel system is considered as *single-carrier* bound and is obtained by:

$$C_{\mathrm{SC}} = \lim_{N\to\infty} W\sum_{n=1}^{N}\frac{1}{N}\log_2\left(1+\frac{\mathrm{SNR}_n}{\Gamma}\right) = W\log_2 \lim_{N\to\infty}\prod_{n=1}^{N}\left(1+\frac{\mathrm{SNR}_n}{\Gamma}\right)^{\frac{1}{N}} \tag{6}$$

The limit can be calculated as,

$$\lim_{N\to\infty}\prod_{n=1}^{N}\left(1+\frac{\mathrm{SNR}_n}{\Gamma}\right)^{\frac{1}{N}} = \exp\left(\lim_{N\to\infty}\sum_{n=1}^{N}\ln\left(1+\frac{\mathrm{SNR}_n}{\Gamma}\right)^{\frac{1}{N}}\right) = \exp\left(\frac{1}{W}\int_0^W \ln\left(1+\frac{\mathrm{SNR}(f)}{\Gamma}\right)df\right) \tag{7}$$

Literally, this limit is related to the so-called Salz SNR, which is often used in practical system implementations to estimate the system noise margin (required SNR subtracted from achievable SNR). The Salz SNR is defined as:

$$\gamma_\infty^W\left\{V(f)\right\} = e^{\frac{1}{W}\int_0^W \ln\left(V(f)\right)df} \tag{8}$$

Therefore,

$$C_{\mathrm{SC}} = W\log_2\gamma_\infty^W\left\{1+\frac{\mathrm{SNR}(f)}{\Gamma}\right\} \tag{9}$$

In fact, this bound indicates the ultimate throughput of a real implementation of a system with finite coding gain and signal processing for any communication medium. One such implementation is the minimum mean-squared error decision feedback equalizer (MMSE-DFE) [7], or Tomlinson-Harashima Precoding (THP) [8][9]. If the individual channels are treated and equalized separately, and the interference signals from other channels are considered as noise (although the power of these interfering signals are attenuate by proper crosstalk cancellers), then the total SISO single-carrier capacity reads as

$$C_{\mathrm{SC}}^{\mathrm{SISO}} = \sum_{n=1}^{4} W\log_2\gamma_\infty^W\left\{1+\frac{1}{\Gamma}\frac{\bar{P}_s\left|\boldsymbol{H}_{n,n}(f)\right|^2}{\sigma_v^2+\bar{P}_s\left(\sum_{l=1,l\neq n}^{4}\left[\Gamma_{nl}^F\left|\mathrm{F}_{n,l}(f)\right|^2+\Gamma_{nl}^N\left|\mathrm{G}_{n,l}(f)\right|^2\right]\right)}\right\} \tag{10}$$

where Γ_{kk}^N, Γ_{kl}^N, and Γ_{kl}^F are attenuation factors of the corresponding RL, NEXT, and FEXT crosstalk cancellers, respectively.

Maximizing the data rate, for a set of parallel channels when the symbol rate is fixed, requires maximization of the achievable $C=\sum_n c_n$ over $\mathcal{E}_n$, the average power of each sub-channel. This is summarized as the following maximization problem, where H_n represents the *n*th sub-channel transfer function.

$$\lim_{N\to\infty}\begin{pmatrix}\underset{\mathcal{E}_n}{\text{maximize}}\; W\sum_{n=1}^{N}\log_2\left(1+\frac{\mathcal{E}_n\left|H_n\right|^2}{\Gamma N_n}\right)\\ \text{subject to}\sum_{n=1}^{N}\mathcal{E}_n = N\mathcal{E}_x\end{pmatrix} \tag{11}$$

where $\mathcal{E}_x$ is the average power of sub-channels. We should mention here that the optimization is done separately for each twisted pair. This corresponds to our previous assumption that twisted pairs are more or less similar. One can perform a joint optimization in case the characteristics of twisted pairs differ significantly. A natural solution of this optimization problem is to use Lagrange multipliers [5]. In this paper, we refer to the maximum value of this function, denoted by C_{WF}, as the *water-filling bound*.

The loss between MIMO and SISO Implementations

In [17], it is shown that in the case of strictly monotonous decreasing channel attenuation, a constant power density in the first Nyquist set of frequencies $f \in [-1/2T, 1/2T]$ is optimum. Therefore, as a generalization of Shannon-Hartley theorem, the capacity of the MIMO system can be evaluated as

$$C_{\text{MIMO}} = \int_0^W \log_2 det\left(\mathbf{I}_{N_T} + \frac{P(f)}{\sigma_v^2}\mathbf{H}(f)\mathbf{H}^\dagger(f)\right)df \qquad (12)$$

where W is the available bandwidth.

It is quite common in practice that in multi-channel systems, the individual channels are equalized independently, and crosstalk terms from other channels are removed by fixed or adaptive cancellers. Therefore, a channel matrix $\mathbf{H}$ can be rewritten as,

$$\mathbf{H} = \mathbf{D} + \mathbf{F} \qquad (13)$$

where $\mathbf{D}$ and $\mathbf{F}$ are the polynomial matrices containing the diagonal and off-diagonal elements of $\mathbf{H}$, respectively (i.e. $\mathbf{D} = diag\{\text{H}_{1,1}, \text{H}_{2,2}, \text{H}_{3,3}, \text{H}_{4,4}\}$ and $\boldsymbol{F} = [\text{H}_{i,j}]_{i \neq j}$).

The decomposition of $\mathbf{H}$ in (13) can be interpreted differently. One can consider this system as a multiple access channel (MAC) with two users, as shown in Fig. 3. If the detection starts with user 1, the maximum rate of this user is [18]

$$C_1 = \int_0^W \log_2 det\left(\mathbf{I}_4 + P(f)\mathbf{D}(f)\mathbf{R}_{vv}^{-1}(f)\mathbf{D}^\dagger(f)\right)df \qquad (14)$$

where $\mathbf{R}_{vv}^{-1} = \sigma_v^2\mathbf{I}_4 + P(f)\mathbf{F}(f)\mathbf{F}^\dagger(f)$ and $\int_0^W P(f) = \bar{P}_s$. Therefore, if the rate of user 1 fulfills $R_1 < C_1$, it can be detected without errors and, hence, removed from the received signal. The remaining signal used by user 2 is now only impaired by the thermal noise, leading to its maximum rate

$$R_2 = C_2 = \int_0^W \log_2 det\left(\mathbf{I}_4 + \frac{P(f)}{\sigma_v^2}\mathbf{F}(f)\mathbf{F}^\dagger(f)\right)df \qquad (15)$$

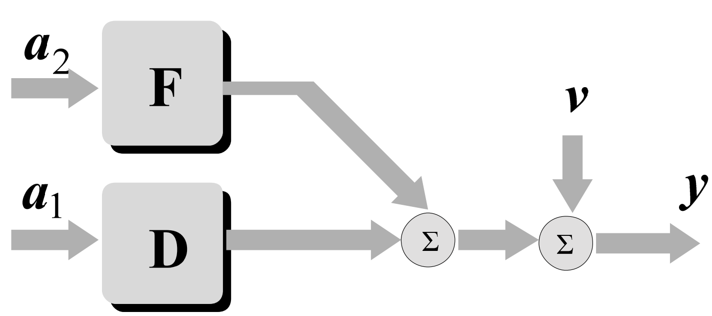

Fig. 3 of H into diagonal and off-diagonal elements
to represent it as a MIMO multiple-access channel.

Recall from multi-user detection theory [18] that $\mathrm{R}_1 + \mathrm{R}_2$ is bounded above by the capacity of the channel, C_{MIMO}. This leads to the conclusion that $\mathrm{R}_1 \le C_{\mathrm{MIMO}} - \mathrm{R}_2$, which means the interference terms must be attenuated enough to achieve high-capacity SISO implementation for user 1. By this method, one can achieve reliable bounds for FEXT attenuation factors, Γ^{F}. A similar approach can be used to determine proper

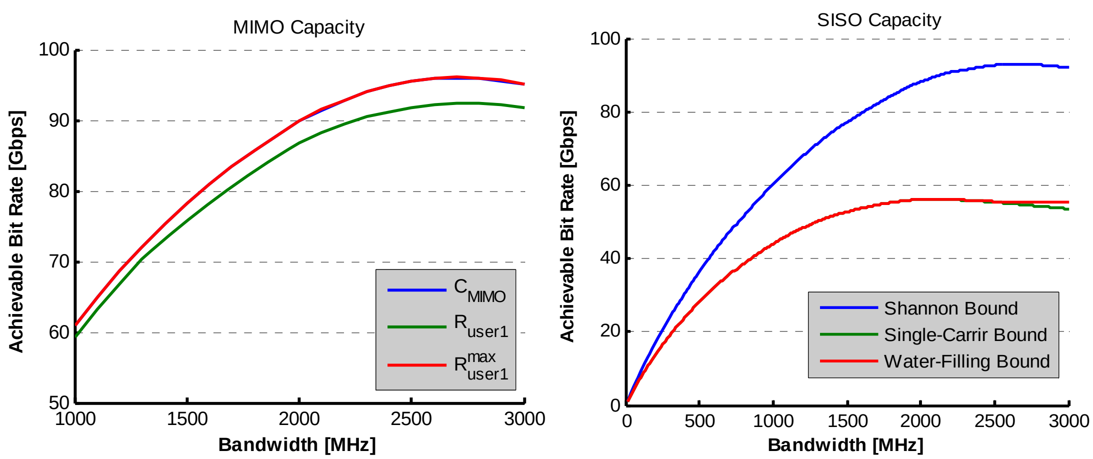

Fig. 4 MIMO capacity and R_1 rate for 50m cable. The SISO Shannon capacity depicted on right is only 3Gbps is less than MIMO capacity.

attenuation levels for NEXT, Γ^{N}.

There are a few remarks about this figure explained as follows. First, the maximum data rate of user 1 is only 3Gbps less than the total MIMO capacity of this channel which indicates the amount of information carried by the FEXT channels is negligible. Second, the SISO capacity of this cable has a maximum of 93Gbps without any FEXT and NEXT cancellation which is about the same as the maximum rate of user 1. This proves that the channels are isolated form each other very well and they perform almost as well as the isolated parallel channels. Finally, despite the fact that the MIMO system outperforms the SISO system, it results in very minor improvement over SISO implementation but at higher cost and power consumption which might not be acceptable.

Rate Optimization

It is of considerable importance to study the problem of input symbol rate optimization under practical realizability constraints. This is especially important for ultra high-speed applications where the trade-offs of power consumption, implementation complexity, and reliability are dramatically challenging. We obtain the optimum specifications for systems equalized by an ideal (no error propagation) infinite-length MMSE-DFE [14][15].

Minimizing the probability of error

Here, we are interested in achieving a fixed target bit rate while keeping the probability of error P_e as small as possible. This can be achieved by performance analysis of the coded system and link budget analysis for DFE implementation. Assume the same signal constellation $\mathcal{A}$, eq. (1) for each individual channel (dimension). Also suppose the power is equally divided among the transmitters. Under these conditions, in CAT-7A cable, it is fairly reasonable to assume same average error probability for individual channels. The average symbol power for this signaling is $\bar{P}_s = \mathsf{E}\{|\,\boldsymbol{x}_k\,|^2\}$ [7] where $\boldsymbol{x}_k$ is drawn form a 4-dimenstional lattice $\mathcal{A}^4$. Consequently, the power of each constituent QAM constellation is $\bar{P}_s\,/\,2$. The union bound estimate of the probability of symbol decoding error associated with each of these constellations is [12]

$$p_e \cong K_{\min} Q\left(\sqrt{3\mathrm{SNR}_{\mathrm{norm}}\gamma_c(\Lambda)\gamma_s(\Lambda)\,/\,\gamma_m}\right) \tag{16}$$

where $K_{\min}$ is the multiplicity of codewords with minimum weight, $\gamma_c(\Lambda)$ is the *nominal coding gain* associated with set partitioning, $\gamma_s(\Lambda)$ is the *shaping gain*, and γ_m is the desired system margin []. The $\mathrm{SNR}_{\mathrm{norm}}$ is the normalized SNR and signifies how far a system is operating from the Shannon limit (the *gap to capacity*). More importantly, this quantity is independent of constellation size for large signal spaces. This, in fact, significantly reduces the underlying analysis. For our QAM baseline, we have $\gamma_s(\Lambda) = 1$ and $\gamma_c(\Lambda) = d_{\min}^2(\Lambda)$. Therefore, p_1 reduces to

$$p_1 = K_{\min} \mathsf{Q}\left(\sqrt{3\mathrm{SNR}_{\mathrm{norm}} \times \frac{d_{\min}^2(\Lambda)}{\gamma_m}}\right) \tag{17}$$

We should recall that the $\mathrm{SNR}_{\mathrm{norm}}$ defined in this section is the same SNR gap Γ used in (6). From (17), it is clear that p_e is minimized when the $\mathrm{SNR}_{\mathrm{norm}}$ is maximized (assuming coding gain and γ_m are fixed). One can calculate the $\mathrm{SNR}_{\mathrm{norm}}$ at each frequency from (9) and put it back into (17) to obtain the error probability versus bandwidth.

Now, we consider two communication systems transporting data at rates 40 and 100Gbps over 20m and 50m, respectively, of horizontal balanced CAT-7A cables. These systems

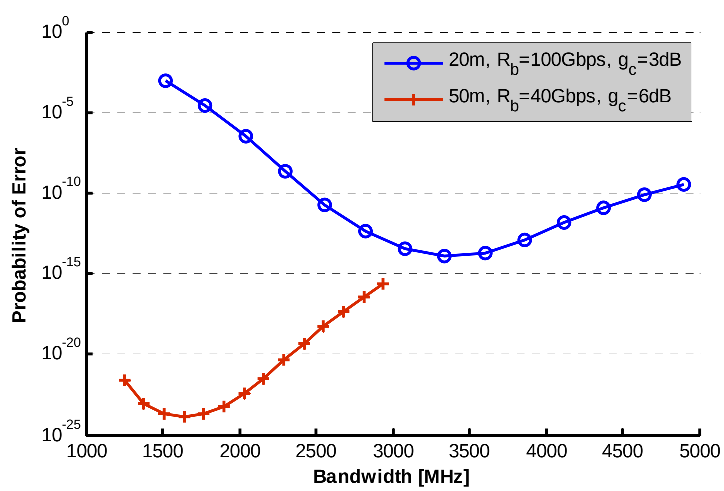

Fig. 5 . Minimization of probability of error through symbol rate optimization for two 40GBASE-T and 100GBASE-T systems.

are equalized by an ideal infinite-length MMSE-DFE. Fig. 5 depicts the variation of p_e as a function of bandwidth W for a target system margin of 0dB. It reveals that the optimum bandwidth values, under probability of error minimization constraint, are 2960 and 1250 MHz, corresponding to 20m and 50m, respectively.

Maximizing the system margin

Alternatively, the system designer may want to choose a specific reliability level, and seek to maximize the system margin to account for unforeseen sources of performance degradation. By rearranging (17), one can define the systems margin in terms of error probability, coding gain, and gap to capacity as

$$\gamma_m = \frac{3\mathrm{SNR}_{\mathrm{norm}} d_{\min}^2(\Lambda)}{\left(Q^{-1}\left(p_1 / K_{\min}\right)\right)^2} \tag{18}$$

This means that, assuming a fixed coding gain, the two optimization scenarios, one that minimizes P_e for fixed γ_m, and the other that maximizes γ_m for fixed p_1, lead to the same optimum bandwidth. In fact, in both cases $\mathrm{SNR}_{\mathrm{norm}}$ is maximized.

The system margins versus bandwidth of the systems considered in the previous section are shown in Fig. 6. As we can see, the system transmitting data at 40Gbps over 50m passes the 6dB margin requirement if a 6dB coding gain is available. A 3dB coding gain for a system transmitting data at 100Gbps can guarantee only a 2dB margin.

We conclude this section by the following remarks. First, the probability of error minimization and margin maximization happen to give the same optimum bandwidth. This is not the case in general as the power minimizing bandwidth of the MMSE-DFE is in general different from the bandwidth that maximizes margin. Second, figures 5 and 6 do not show any symmetry about the optimum bandwidth. More precisely, one can, in general, over-estimate the optimal bandwidth by a few percent (the flatness of curves around optimum point differ in different scenarios) instead of under-estimating it, without any serious degradation. Finally, it is apparent from Figs. 5 and 6 that the DFE can suffer

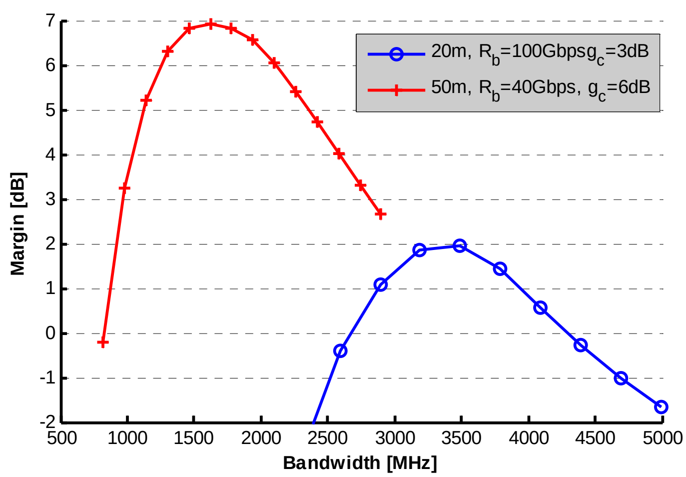

Fig. 6 Maximization of margin for two 40GBASE-T and 100GBASE-T systems.

significant performance degradation when the transmission bandwidth is not optimized. Therefore, for high data rate applications, the process of rate optimization becomes extremely important.

Signal Design

Last section revealed the importance of rate optimization to find out the optimum bandwidth and a coding technique that can achieve a given reliability. From the required coding gain one can determine a class of coding scheme and design a proper code. It is known from the classic coding theory that a coding gain up to 5dB is achievable by trellis coded modulation at reasonable complexity. A simple but yet powerful outer Reed-Solomon code can improve this by another 1dB but at the cost of minor bandwidth expansion. Higher coding gain can be obtained by more complex low-density parity-check (LDPC) or turbo codes.

Trellis coded modulation, in spite of its limited coding gain, offers a compact, low-power and low-latency decoding which can be combined with decision feedback equalizer to eliminate error propagation by replacing the tentative decision with more reliable ones in feedback path. This method exploits the survivor path memory of a Viterbi decoder containing the reliable decisions in feedback path, and it is called *survivor path feedback equalizer* (SPFE) [ ]. Malhotra et. al. extended the SPFE concept for multi-dimensional TCM applicable in multiple channel communications, and also employed soft and hard iterative DFE as more protection against error propagation of DFE [ ]. This is shown in Fig. 7.

For higher coding gains, we follow the structure of the block coded modulation adopted for 10GBASE-T, and try to generalize the formulations. The goal is to design a high-rate high-gain coding scheme form a low-rate powerful code. Suppose that g_c denotes the minimum required coding gain. An $[\mathcal{N}, \mathcal{K}]$ block code, either systematic or nonsystematic, operating in the *waterfall region* is considered here. We construct the transmit symbols as follows. A block of $\mathcal{K}$ data bits is coded into $\mathcal{N}$ coded bits, and arranged into a block with n_r rows and n_c columns (If $\mathcal{N} \neq n_r.n_c$ a few dummy bits can

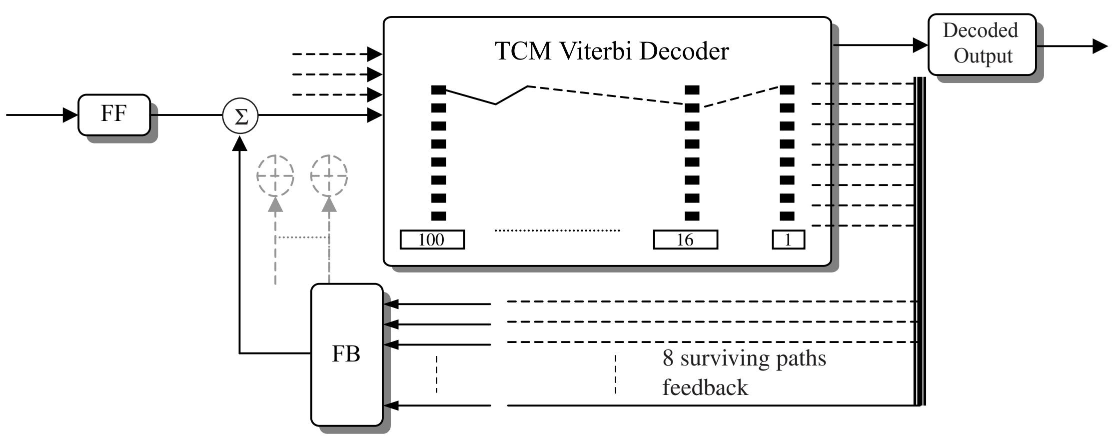

Fig. 7

be inserted, therefore we assume $\mathcal{N} = n_r.n_c$ hereafter). Another block of $n_a.n_c$ uncoded bits are stacked to the block of coded bits. Then every group of $n_a + n_r$ bits, read column wise from the constructed block, is mapped to one signal point in a two dimensional constellation $\mathcal{X}$, e.g., QAM constellation. The real and imaginary parts of signal points are assigned to two twisted-pairs. The signal points obtained from this constructed block can be assigned to the other tow pairs alternately, or another block can be constructed and is assigned to the remaining pairs. The results yield a 4-dimensional signal $\boldsymbol{x}_k$. We denote the cardinality of the QAM constellation as $|\mathcal{X}|$. The total rate of this coding scheme is

$$r_t = \frac{\mathcal{K} + n_a.n_c}{\mathcal{N} + n_a.n_c} > r_C = \frac{\mathcal{K}}{\mathcal{N}} \tag{19}$$

where r_C is the rate of the original block code.

The signal space $\mathcal{X}$ is partitioned into a number of cosets Λ by set partitioning rules [13], such that $\delta_l^2 \le g_c \le \delta_{l+1}^2$, where δ_l^2 is the minimum intraset distance at partitioning level l . The coded bits are used for coset selection and uncoded bits select the signal points in each coset. This requires $n_r \ge l + 1$ guaranteeing the overall coding gain of g_c. To determine n_a , assume that a target bit rate of R_b is desired. If a total bandwidth of W is available, the maximum deliverable symbol rate without intersymbol interference is $R_{sym} = 2W / (1 + \alpha)$ where α is the roll-off factor of pulse-shaping filter. Hence, the number of bits sent by each symbol is $n_b = R_b / R_{sym}$. Then, the cardinality of 4-dimensional space supporting this coded system reads as

$$\mathscr{N} = |\mathcal{X}|^2 \ge 2^{n_b/r_t} = 2^{R_b(1+\alpha)/2Wr_t} \tag{20}$$

Therefore, if we restrict ourselves to rectangular 2-dimentional lattices, n_r can be determined from $|\mathcal{X}| \ge 2^{n_r+n_a}$. Unfortunately, the parameter r_t in the right-hand side of (20) is implicitly a function of n_r . This can be resolved by the following rather simple algorithm. The algorithm starts initializing the total rate with roughly a small value. This

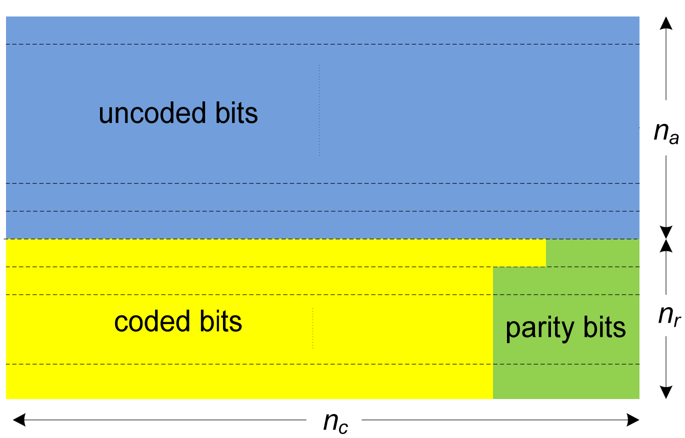

Fig. 8 Construction of block coded modulation.

will simply overestimate n_r, to make sure that the signal constellation is large enough to accommodate all the $2^{n_b/r_t}$ signal points. Then, the actual rate is calculated according to (19), and an upper bound for n_a is obtained, i.e., $n_b / (2r_t) - n_r$. If n_r falls under this constraint, then the algorithm stops, otherwise n_r is decreased one unit and the rate gets updated. This procedure continues until a value of n_a that satisfies all the constraints is obtained.

A block coded system for 40GBASE-T system over 50m is designed for up to 8dB coding gain. A 9dB set partitioning is performed on a 2-dimenstional lattice. Suppose the bandwidth is set to 1350MHz. Using LDPC(1024, 833), which is proven to achieve coding gain more than 8dB and no error floor up to 10^{-13} [19], results in a constituent 324-QAM constellation (18-PAM per real dimensional), where a pulse shaping filter with 8% roll-off factor is used. A bandwidth of 1410MHz, assuming the other parameters are fixed, will result in 256-QAM, that may offer slightly lower margin but less complexity in terms of mapper and demapper design.

Algorithm 1.

1: initialize $r_t = 0.5$;

2: set $|\mathcal{X}|^2 = 2^{n_b/r_t}$;

3: $n_a = \lfloor \log_2 |\mathcal{X}| - n_r \rfloor$;

4: update r_t according to the block coded modulation: $r_t = (\mathcal{K} + n_a.n_c)/(\mathcal{N} + n_a.n_c)$

5: if $n_a \le n_b / (2r_t) - n_r$

exit;

else

$n_a \leftarrow n_a - 1$;

update r: $r_t = (\mathcal{K} + n_a.n_c)/(\mathcal{N} + n_a.n_c)$;

end

6: goto 2

Conclusions

In this paper, we presented the technical feasibility of beyond 10Gbps high-speed transmission over standard Category 7A copper wire. Our assessments have revealed that CAT-7A cables are, theoretically, capable of delivering data stream at a speed of 40bps over 50m thanks to their excellent shielding and engineering design. Also, based on our modeling and analysis, the maximum achievable rate over 20m cables is well above 100Gbps. However, with various degrees of DSP, the objective of running 100GBASE-T over CAT-7A cable can be achieved with some effort by the silicon vendors, probably in the next generations of CMOS technology. We conclude that 40GBASE-T is practical over 50m of CAT-7A cable, and this is within the realm of expectation of current objectives of IEEE standard committee.

ACKNOWLEDGMENT

The authors gratefully acknowledge the kind support and helpful discussions with Nexans's engineers and the tools and services of CICTR and high performance computing services at The Pennsylvania State University.

References

1. IEEE 802.3 Higher Speed Study Group Objectives, July 2007.
2. M. Kavehrad, J. F. Doherty, J. H. Jeong, A. Roy and G. Malhotra, “10 Gbps Transmission over Standard Category-5 Copper Cable”, *Proceedings of IEEE GLOBECOM’03*, San Francisco – CA., December 2003.
3. Sallaway, *10GBASE-T Channel Criteria*, IEEE 802.3 10GBASE-T Study Group Interim Meeting. Portsmouth, NH, May 21 − 22, 2003.
4. J.H. Conway and N.J.A. Sloane, *Sphere Packings, Lattices and Groups*, Springer, 1998.
5. R. E. Blahut, Principles and Practice of Information Theory. Addison-Wesley, 1987.
6. I. Kalet and S. Shamai, “On the capacity of a Twisted-Wire Pair: Gaussian Model”, *IEEE Transactions on Communications*, vol. 38, No 3, March 1990.
7. J. Proakis, Digital Communications. McGraw-Hill, August 2000.
8. M. Tomlinson, “New automatic equalizer employing modulo arithmetic,” *Electron. Lett.*, vol. 7, pp. 138–139, Mar. 1971.
9. H. Harashima, H. Harashima, and H. Miyakawa, “Matched-Transmission Technique for Channels With Intersymbol Interference,” *Communications, IEEE Transactions on*, vol. 20, 1972, pp. 774-780.
10. H. Jafarkhani, Space-Time Coding: Theory and Practice, Cambridge University Press, 2005.
11. G. Malhotra, J. H. Jeong and M. Kavehrad, “Joint MIMO Equalization and Decoding for 10GBASE-T Transmission,” *Proceedings of GLOBECOM’04*, Dallas Texas, November 2004.
12. G.D. Forney, G. Ungerboeck, Modulation and Coding for Linear Gaussian Channels, IEEE Transactions on Information Theory, Vol. 44, Issue 6, pp. 2384 − 2415, Oct 1998.
13. G. Ungerboeck, “Trellis-Coded Modulation with Redundant Signal Sets - I: Introducation”, *IEEE Communications Magazine*, vol. 25, pp. 5-11, 1987.
14. Fischer, Robert F.H. “MMSE DFE for High-Rate MIMO Transmission Over Channels With ISI”, *Fifth IEE International Conference on 3G Mobile Communication Technologies*, pp. 83-87, London, United Kingdom Oct 2004.
15. R. Fischer, J. Huber, G. Komp, “Coordinated Digital Transmission: Theory and Examples”, *Archiv für Elektronik und Übertragungstechnik, Internat. J. Electron. Com,* Vol.48, No. 6, pp. 289-300, Nov. 1994.

16. M. Kavehrad and J. Salz, Cross-Polarization Cancellation and Equalization in Digital Transmission Over Dually-Polarized Multipath Fading Channels, *AT&T Technical Journal*, Vol. 64, No. 10, Dec. 1985.
17. R. Price, "Nonlinear Feedback Equalized PAM Versus Capacity for Noisy Filter Channels", *in Proc. of IEEE International Conference on Communications (ICC)*, Philadelphia, PA, June 1972, pp. 22.12-22.17.
18. S. Verdú, *Multiuser Detection*, Cambridge University Press, 1998.
19. K. Seki, *et. al.*, Performance Evaluation of Low-Latency LDPC Code, IEEE 802.3 10GBASE-T Study Group Interim Meeting, July 2004.